JACS
JOURNAL OF THE AMERICAN CHEMICAL SOCIETY
Communication
pubs.acs.org/JACS

Solid-State Magnetic Switching Triggered by Proton-Coupled Electron-Transfer Assisted by Long-Distance Proton-Alkali Cation Transport

Pauline Higel,[†] Françoise Villain,[†] Michel Verdaguer,[†] Eric Rivière,[‡] and Anne Bleuzen*[,‡]

[†]Institut Parisien de Chimie Moléculaire, Université Pierre et Marie Curie, UMR CNRS 8232, Case 42, 4 place Jussieu, 75252 Paris Cedex 05, France

[‡]Institut de Chimie Moléculaire et des Matériaux d'Orsay-Equipe de Chimie Inorganique, Université Paris-Sud, UMR CNRS 8182, 91405 Orsay, France

Supporting Information

ABSTRACT: Acidity of water molecules coordinated to Co ions in CoFe Prussian blue analogues (PBA) has been used to reversibly activate the $Co^{III}Fe^{II} \leftrightarrow Co^{II}Fe^{III}$ electron transfer. The study of the structure and the electronic structure shows that the process implies an original PCET reaction between a solid-state porous coordination polymer and hydroxide ions in solution. The PCET reaction spreads throughout the solid network thanks to a long-range H^+ and Rb^+ transport within the pore channels of PBA taking advantage of the hydrogen-bonding network of zeolitic water molecules acting as proton wires.

The interaction between protons and electrons plays a central role in chemistry and in biology as proton-coupled electron transfer (PCET) reactions are involved in many chemical and natural processes.[1] The PCET reactions also constitute a key point in contemporary challenges such as energy conversion.[2] They have been intensively studied in solutions, proteins, and electrochemistry.[3] Most of the studies aim at a better understanding of the mechanisms that underlie the efficiency of PCET reactions and most of them focus on solutions. In this work instead, we report an original PCET reaction in a system composed of a solid-state porous coordination polymer (a Prussian blue analogue, PBA) immersed in an aqueous solution. The acid−base reaction results in the magnetic switching of the solid network between a ferrimagnetic state and a paramagnetic state.

Some three-dimensional coordination polymers undergo a reversible electron transfer under external strain.[4−14] Thus, in some CoFe Prussian blue analogues (CoFe PBA in the following) presenting the well-known face-centered cubic (fcc) structure[15] made of Co-NC-Fe linkages, the switch between the Co^{III}(LS; low spin)-NC-Fe^{II}(LS) and the Co^{II}(HS; high spin)-NC-Fe^{III}(LS) states can be activated by light,[6,8] temperature,[16,17] or pressure.[18,19] The switching properties depend, among other parameters, on the relative energy levels of the $Co^{III}Fe^{II}$ and $Co^{II}Fe^{III}$ states, which are related to the relative position of the redox potentials of the Co^{III}/Co^{II} and Fe^{III}/Fe^{II} redox couples.[20] In CoFe PBAs, chemical modification of the Fe ion coordination sphere is not feasible since iron is strongly covalently linked to six C-bonded cyanide bridges. The low spin state is very stable. On the contrary, the coordination sphere of the Co ions is described as $[Co(NC)_y(OH_2)_{(6-y)}]$. It contains coordinated water molecules making these metallic sites accessible to acid−base reactions.[15] This allows to tune the redox properties of the Co site. The alkali-cation free CoFe PBA has the chemical formula $Co_4[Fe(CN)_6]_{2.7}\square_{1.3}\cdot 18H_2O$, where $\square$ stands for the $[Fe(CN)_6]$ vacancies. It can be reformulated $(Co(OH_2)_2)_4[Fe(CN)_6]_{2.7}\square_{1.3}\cdot 10H_2O$ to highlight the coordinated molecules on the cobalt if one ignores minority species presenting one- or three-coordinated water molecules. It is made of Co^{II}(HS) and Fe^{III}(LS) ions linked by cyanide and does not exhibit any switching properties at ambient pressure.[8] In order to reach the Co^{III}(LS)-Fe^{II}(LS) state, one has to increase the reducing power of the Co ion (i.e., decrease its redox potential). We show in the present contribution that this can be achieved through a local PCET reaction accompanied by a long-distance proton and alkali-cation transport within the pores of the inorganic network. The reversibility of the reaction is checked, and the way the reaction propagates throughout the solid is investigated.

Insoluble alkali cation free CoFe PBA is called compound **1** in the following. It was immersed in a concentrated rubidium nitrate aqueous solution, and increasing volumes of a tetrapropylammoniumhydroxide (TPAOH) aqueous solution were added. The precise amount of reactants is given in Table S1. Up to a TPAOH/Co mole ratio threshold (TPAOH/Co mole ratio $\leq$0.6), the pH of the solution remained unchanged, showing that the added hydroxide ions are consumed by acid−base reaction with the solid. By increasing the TPAOH/Co mole ratio above 0.6, the pH of the solution rapidly increased and then reached a maximum. The corresponding powder (TPAOH/Co = 3.5) was recovered after 5 min of vigorous stirring. It is called compound **2** in the following. The chemical composition of **1** and **2** deduced from elemental analyses (Table S2) are as follows: $(Co(OH_2)_2)_4[Fe(CN)_6]_{2.7}\cdot 10H_2O$ for **1**[8] and $Rb_{2.5}(Co(OH)(OH_2))_{2.5}(Co(OH_2)_2)_{1.5}[Fe(CN)_6]_{2.7}\cdot 10.5H_2O$ for **2**. We identify in the formula of **2** the cobalt sites where some of the water coordinated molecules have lost a proton to become hydroxo ligands. The same Co:Fe

Received: March 6, 2014
Published: April 14, 2014

   dx.doi.org/10.1021/ja502294x | J. Am. Chem. Soc. 2014, 136, 6231−6234

stoichiometry in both compounds indicates that the acid−base reaction did not significantly modify the bimetallic cyano-bridged network. The elemental analyses data are fairly well reproduced by considering the hydroxylation of 2.5 water molecules accompanied by the insertion of 2.5 Rb^+ cations per cell to ensure electroneutrality of the solid. In other words, 2.5 protons of water molecules bound to the Co sites of the inorganic polymer have been consumed by acid−base reaction with TPAOH, while the negative charge borne by the inorganic network is compensated by the insertion of 2.5 Rb^+ cations within the PBA porous channels (Scheme 1), i.e., in the octants

Scheme 1. Acid−Base Reaction between the Solid Inorganic Network and Hydroxide Solution Accompanied by the Insertion of Rb^+ Cations within the Porous Channels of PBA

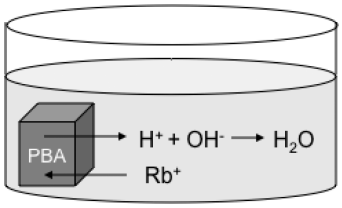

of the PBA conventional cell. The structural and electronic modifications of the CoFe cyanide bimetallic network accompanying the acid−base reaction were studied by X-ray diffraction (XRD), X-ray absorption spectroscopy (XAS), and magnetometry in compounds **1** and **2**.

The XRD patterns, the magnetization curves and the XAS spectra at the Co K-edge of compounds **1** and **2** are shown in Figure 1a−c. The XRD pattern of compound **1** is the signature of the well-known fcc structure of alkali-cation free PBAs (Figure 1a)[15] with a cell parameter value (10.30 ± 0.05 Å) typical of CoFe PBAs mainly composed of Co^{II}(HS) ions with long Co to ligand bonds.[8] Compound **1** presents a long-range ferrimagnetic ordering below the Curie temperature T_C = 16 K (Figure 1b).[8] The absorption maximum at 7725 eV at the Co K-edge on the spectrum of compound **1** (Figure 1c) is the signature of divalent Co^{II}(HS) in CoFe PBAs.[8,17,21−23] The XRD pattern of **2** shows the same peaks than **1**: the long-range fcc structure is not changed by the acid−base reaction. The strong decrease in intensity of the 200 and the 420 diffraction lines from compound **1** to **2** reflects an increase of electronic density at the center of the octants, which is the usual position of interstitial Rb^+ metal ion in PBAs.[17] This reveals the location of the Rb^+ ions inserted within the PBA pore channels during the acid−base reaction. At last, the shift of the peaks indicates a cell parameter contraction from compound **1** (10.30 ± 0.05 Å) to compound **2** (10.00 ± 0.05 Å). Such an important contraction is observed in CoFe PBAs when Co^{II}(HS) ions with long Co to ligand bonds (2.08 Å) are transformed into Co^{III}(LS) ions with short Co to ligand bonds (1.96 Å).[8] The spectacular magnetization decrease from compound **1** to **2** (Figure 1b) is in agreement with the local transformation of paramagnetic Co^{II}(HS)Fe^{III}(LS) (S = 1) pairs into diamagnetic Co^{III}(LS)Fe^{II}(LS) (S = 0) ones and with the associated transformation of a long-range ordered ferrimagnetic phase to a paramagnetic one below T_C.[8] The oxidation states of the metal ions were confirmed by XAS. At the Fe K-edge (Figure S3), the shift of the absorption maximum (1s → 4p transition) by 1 eV toward low energy after addition of base is the signature of a decrease of the oxidation state of most of the Fe ions from Fe^{III}

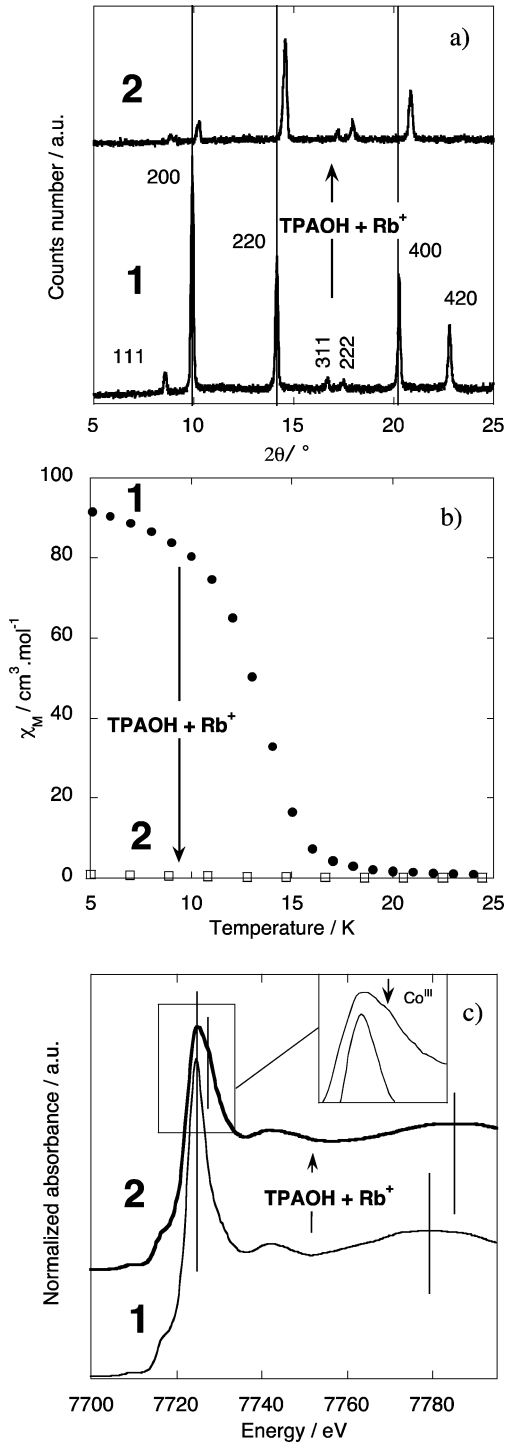

Figure 1. (a) Powder XRD patterns, (b) temperature dependence of the molar magnetic susceptibility, and (c) Co K-edge X-ray Absorption Near Edge Structure spectra for compounds **1** and **2**. The arrow in the inset points at the shoulder (see text).

to Fe^{II} demonstrated in other contexts in CoFe PBAs.[8,17,21−23] It is confirmed by infrared spectroscopy (Figure S4).[17,24−26] The Co K-edge spectrum of **2** (Figure 1c) shows a broader 1s → 4p absorption band than compound **1**. The maximum situated at 7725 eV indicates that compound **2** contains Co^{II}(HS) ions embedded in the same environment as in compound **1** ($Co^{II}(NC)_4(OH_2)_2$). Given the stoichiometry, a Co^{II}(HS) contribution is indeed expected in compound **2** since

dx.doi.org/10.1021/ja502294x | J. Am. Chem. Soc. 2014, 136, 6231−6234

it only contains 2.7 CoFe pairs per cell possibly involved in the $Co^{II}Fe^{III} \rightarrow Co^{III}Fe^{II}$ charge transfer. A significant shoulder at higher energy (around 7727 eV) is the signature of another Co species assignable to Co^{III}(LS) ions. The Co^{II}(HS) to Co^{III}(LS) transformation is confirmed by the significant shift of the first extended X-ray absorption fine structure oscillation toward higher energy consistent with the Co to ligand bond shortening accompanying the Co^{II}(HS) → Co^{III}(LS) transformation.

The fraction of $Co^{III}Fe^{II}$ pairs in compound **2** can be estimated from the linear fit of the inverse molar magnetic susceptibility ($1/\chi_M$) versus T over the 100−300 K temperature range (Figure S5).[18] Given the error bars, the presence of 2.3 (±0.2) $Co^{III}Fe^{II}$ diamagnetic pairs per cell in **2** is in line with the reduction of the main part of the Fe ions and fairly well corresponds to the 2.5 hydroxylated Co species per cell. Compound **2** can then be depicted as mainly composed of hydroxylated HO-Co^{III}(NC)Fe^{II} linkages and non-deprotonated H_2O-Co^{II} species. These observations allow to reach two important conclusions (i) on the PCET mechanism and (ii) on the magnetism. First conclusion, the acid−base reaction and the $Co^{II}Fe^{III} \rightarrow Co^{III}Fe^{II}$ electron transfer are coupled, the Co^{II}−OH_2 sites acting at the same time both as proton donor toward OH^- proton acceptors provided by the TPAOH solution and as electron donor toward Fe^{III} electron acceptor sites of the coordination polymer. The fact that only the Co species implied in the electron transfer are hydroxylated suggests a concerted proton−electron transfer (CPET) rather than a stepwise proton−electron transfer (PET) mechanism: hydroxide ions in the pore channels attack the H atoms of the weakly acidic water molecules bound to the Co^{II} ions, which reinforces the H_2O to Co^{II} σ donation and lowers the Co^{III}/Co^{II} redox potential enough to trigger the $Co^{II}Fe^{III} \rightarrow Co^{III}Fe^{II}$ electron transfer. The Co^{II} to Co^{III} oxidation enhances the acidity of the water molecules bound to the Co ions implied in the electron transfer and makes easier the deprotonation reaction. It is worth noticing that PCET reactions involving the $[Co^{III}$-$OH]^{2+}/[Co^{II}$-$OH_2]^{2+}$ couple are scarce.[27] A scheme of the chemical equation of the CPET reaction is proposed in Scheme 2. Second conclusion, the magnetism of **2** can be described by

Scheme 2. Schematic Chemical Equation of the PCET Reaction

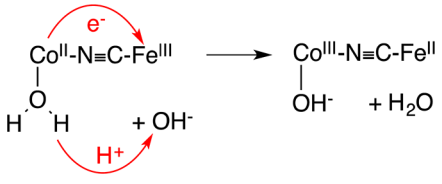

paramagnetic Co^{II} ions, isolated in a diamagnetic $Co^{III}Fe^{II}$ matrix, providing a paramagnetic phase in the whole temperature range.

In order to check if the process could be reversed, **2** was immersed in a concentrated nitric acid aqueous solution (Table S1). The collected precipitate is called compound **3** in the following. The chemical formula (Table S6), XRD pattern (Figure S7), XAS spectra (Figure S8), and magnetization curve (Figure S9) of **3** are very close to those of compound **1** indicative that the system is almost coming back to the initial point.

To explore more precisely the transformation of the system from **1** to **2** and then from **2** to **3**, we prepared intermediate compounds by adding, first, increasing volumes of TPAOH solution (from **1** to **2**) and then increasing volumes of HNO_3 solution (from **2** to **3**) (Table S1). XRD patterns of the intermediates are shown in Figure 2a, and the corresponding

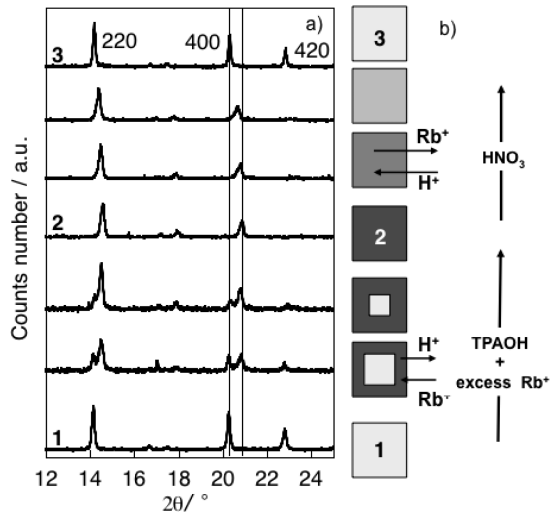

Figure 2. (a) Powder XRD pattern and (b) scheme of the proposed distribution of phases in the particles when going (bottom-up) from **1** to **2** by increasing the amount of TPAOH base, in the presence of an excess of Rb^+ and then when going from **2** to **3** by increasing the amount of nitric acid, in absence of Rb^+. Light gray: phase **1**, $Co_4[Fe(CN)_6]_{2.7}\cdot 18H_2O$; dark gray, phase **2** $Rb_{2.5}Co_4[Fe(CN)_6]_{2.7}(OH)_{2.5}\cdot 16H_2O$; mean gray, single phased $Rb_xCo_4[Fe(CN)_6]_{2.7}(OH)_x\cdot nH_2O$; light gray, phase **3**, $Rb_{0.3}Co_4[Fe(CN)_6]_{2.8}\cdot 24H_2O$. Dark gray + light gray, coexistence of two phases, $x\cdot$**2** (shell) and $(1-x)\cdot$**1** (core).

magnetization curves are shown in Figures S9 and S10. For increasing volumes of base, two peaks appear for each reflection, situated at the same angle than the corresponding peak of **1** and **2**, respectively. The intermediate compounds appear therefore composed of two phases; one close to compound **1** with a large cell parameter mainly composed of Co^{II}(HS) and Fe^{III} ions and the other close to compound **2** with a shorter cell parameter containing Co^{III}(LS) and Fe^{II} ions. As the amount of base increases, the intensity of the peaks at higher angles increases, while the intensity of the ones at lower angles decreases. On the contrary, for increasing amount of acid from compound **2** to compound **3**, only one diffraction peak for each reflection appears, and the peaks are progressively shifted toward lower angles. Only one phase is present; with a continuously increasing cell parameter. Such a behavior is explained by the slow migration of the bulky Rb^+ cations within the solid. High proton conductivity has already been evidenced in comparable compounds and explained by a Grotthus mechanism mediated by the 3D hydrogen-bonding network of zeolitic water molecules filling the porous channels,[26] but the diffusion of bulky hydrated Rb^+ cations constitutes a limiting step. For increasing amount of base from compound **1** to compound **2**, the external shell of the particles undergoes the PCET reaction and is mainly composed of Co^{III} and Fe^{II} ions, whereas the core still mainly contains Co^{II} and Fe^{III} ions, in line with the splitting into two of the diffraction lines. The front propagation of the reaction, limited by the Rb^+ cations migration, moves from the surface to the core of the particles with increasing amount of base, in line with the relative

dx.doi.org/10.1021/ja502294x | J. Am. Chem. Soc. 2014, 136, 6231−6234

intensities of the two peaks. For increasing amount of acid from compound **2** to compound **3**, the reverse PCET reaction is accompanied by the slow and progressive migration of the Rb^+ ions at the same speed throughout the whole solid, in line with a progressive and homogeneous reverse PCET over the whole sample and the uniform and continuous cell expansion.

In conclusion, we show here an original PCET reaction implying a solid-state porous coordination polymer and hydroxide ions in solution. The PCET reaction involves an electron transfer within the polymer network resulting in a reversible switch of the magnetic properties and a proton transfer between accessible coordination sites of the polymer and water confined within its nanoporosity. The PCET reaction spreads throughout the solid network thanks to a long-distance H^+ and Rb^+ transport within the porous channels of PBA taking advantage of the hydrogen-bonding network of zeolitic water molecules acting as proton wires. The slow migration of Rb^+ ions ensures the electroneutrality of the solid, governs the migration of the charged species, and therefore controls the PCET reactions. Hence, the pH of the surrounding medium controls the PCET reaction, the local switch between paramagnetic $Co^{II}Fe^{III}$ pairs and diamagnetic $Co^{III}Fe^{II}$ ones and finally the long-range magnetic order below T_C.

To our knowledge, this is the first example of PCET reactions in a porous coordination polymer with such spectacular changes in the magnetism. The evidence of such a phenomenon offers new perspectives for the study of PCET reactions and long-distance transport of cations in confined media. This also opens a new strategy for the direct coupling of porous properties and magnetic switching.[28]

■ ASSOCIATED CONTENT

Ⓢ Supporting Information

Samples preparation, experimental details, spectroscopic, magnetic and structural data. This material is available free of charge via the Internet at http://pubs.acs.org.

■ AUTHOR INFORMATION

Corresponding Author

anne.bleuzen@u-psud.fr

Notes

The authors declare no competing financial interest.

■ ACKNOWLEDGMENTS

We thank the CNRS, University Paris-Sud, the European community (contract NMP3-CT-2005-515767 NoE "MAGMANET") and the GDR (Magnétisme et Commutation Moléculaire) for financial support.

■ REFERENCES

(1) (a) Stubbe, J.; Nocera, D. G.; Yee, C. S.; Chang, M. C. Y. *Chem. Rev.* **2003**, *103*, 2167. (b) Meyer, T. J.; Huynh, M. H. V.; Thorp, H. H. *Angew. Chem., Int. Ed.* **2007**, *46*, 5284.

(2) (a) Bard, A. J.; Fox, M. A. *Acc. Chem. Res.* **1995**, *28*, 141. (b) Gust, D.; Moore, T. A.; Moore, A. L. *Acc. Chem. Res.* **2009**, *42*, 1890. (c) Hammes-Schiffer, S. *Acc. Chem. Res.* **2009**, *42*, 1881−1889.

(3) (a) Huynh, M. H. V.; Meyer, T. J. *Chem. Rev.* **2007**, *107*, 5004. (b) Costentin, C.; Robert, M.; Savéant, J. M. *Acc. Chem. Res.* **2010**, *43*, 1019. (c) Cukier, R. I.; Nocera, D. G. *Annu. Rev. Phys. Chem.* **1998**, *49*, 337. (d) Mayer, J. M.; Rhile, I. J. *Biochim. Biophys. Acta* **2004**, *1655*, 51.

(4) Kahn, O.; Martinez, C. J. *Science* **1998**, *279*, 44.

(5) Ohba, M.; Yoneda, K.; Agusti, G.; Munoz, M. C.; Gaspar, A. B.; Real, J. A.; Yamasaki, M.; Ando, H.; Nakao, Y.; Sakaki, S.; Kitagawa, S. *Angew. Chem., Int. Ed.* **2009**, *48*, 4767.

(6) Sato, O.; Iyoda, T.; Fujishima, A.; Hashimoto, K. *Science* **1996**, *272*, 704.

(7) Verdaguer, M. *Science* **1996**, *272*, 698.

(8) Bleuzen, A.; Lomenech, C.; Escax, V.; Villain, F.; Varret, F.; Cartier dit Moulin, C.; Verdaguer, M. *J. Am. Chem. Soc.* **2000**, *122*, 6648.

(9) Goujon, A.; Roubeau, O.; Varret, F.; Dolbecq, A.; Bleuzen, A.; Verdaguer, M. *Eur. J. Phys. B* **2000**, *14*, 115.

(10) Ohkoshi, S.; Tokoro, H.; Hashimoto, K. *Coord. Chem. Rev.* **2005**, *249*, 1830.

(11) Cobo, S.; Fernandez, R.; Salmon, L.; Molnar, G.; Bousseksou, A. *Eur. J. Inorg. Chem.* **2007**, 1549.

(12) Buschmann, W. E.; Ensling, J.; Gütlich, P.; Miller, J. S. *Chem.—Eur. J.* **1999**, *5*, 3019.

(13) Coronado, E.; Jiménez-Lopez, M. C.; Korzeniak, T.; Levchenko, G.; Romero, F. M.; Segura, A.; Garcia-Baonza, V.; Cezar, J. C.; de Groot, F. M. F.; Milner, A.; Paz-Pasternak, M. *J. Am. Chem. Soc.* **2008**, *130*, 15519.

(14) Dei, A. *Angew. Chem., Int. Ed.* **2005**, *44*, 1160.

(15) Lüdi, A.; Güdel, H. U. *Structure and Bonding*; Springer-Verlag: Berlin, 1973, pp 1−21 and refs herein.

(16) Sato, O.; Einaga, Y.; Fujishima, A.; Hashimoto, K. *Inorg. Chem.* **1999**, *38*, 4405.

(17) Escax, V.; Bleuzen, A.; Cartier dit Moulin, C.; Villain, F.; Goujon, A.; Varret, F.; Verdaguer, M. *J. Am. Chem. Soc.* **2001**, *123*, 12536.

(18) Ksenofontov, V.; Levchenko, G.; Reiman, S.; Gütlich, P.; Bleuzen, A.; Escax, V.; Verdaguer, M. *Phys. Rev. B* **2003**, *68*, 024415.

(19) Bleuzen, A.; Cafun, J.-D.; Bachschmidt, A.; Verdaguer, M.; Münsch, P.; Baudelet, F.; Itié, J.-P. *J. Phys. Chem. C* **2008**, *112*, 17709.

(20) Cafun, J.-D.; Champion, G.; Arrio, M.-A.; Cartier dit Moulin, C.; Bleuzen, A. *J. Am. Chem. Soc.* **2010**, *132*, 11552.

(21) Yokoyama, T.; Ohta, T.; Sato, O.; Hashimoto, K. *Phys. Rev. B* **1998**, *58*, 8257.

(22) Yokoyama, T.; Kiguchi, M.; Ohta, T.; Sato, O.; Einaga, Y.; Hashimoto, K. *Phys. Rev. B* **1998**, *60*, 9340.

(23) Cartier dit Moulin, C.; Villain, F.; Bleuzen, A.; Arrio, M.-A.; Sainctavit, P.; Lomenech, C.; Escax, V.; Baudelet, F.; Dartyge, E.; Gallet, J. J.; Verdaguer, M. *J. Am. Chem. Soc.* **2000**, *122*, 6653.

(24) Reguera, E.; Bertran, J. F.; Diaz, C.; Blanco, J.; Rondon, S. *Hyperfine Interact.* **1990**, *53*, 391.

(25) Bertran, J. F.; Pascual, J. B.; Hernandez, M.; Rodriguez, R. *React. solids* **1988**, *5*, 95.

(26) Ohkoshi, S. I.; Nakagawa, K.; Tomono, K.; Imoto, K.; Tsunobuchi, Y.; Tokoro, H. *J. Am. Chem. Soc.* **2010**, *132*, 6620.

(27) Wasylenko, D. J.; Ganesamoorthy, C.; Borau-Garcia, J.; Berlinguette, C. P. *Chem. Commun.* **2011**, *47*, 4249.

(28) Maspoch, D.; Ruiz-Molina, D.; Veciana, J. *Chem. Soc. Rev.* **2007**, *36*, 770.